Article

Syntheses and Applications of Symmetrical Dinuclear Half-Sandwich Ruthenium(II)–Dipicolinamide Complexes as Catalysts in the Transfer Hydrogenation of Ketones

Robert Tettey Kumah, Sabathile Thandeka Mvelase and Stephen Otieno Ojwach *

School of Physics and Chemistry, University of KwaZulu-Natal, Pietermaritzburg Campus, Private Bag X01, Scottsville 3209, South Africa
* Correspondence: ojwach@ukzn.ac.za

Abstract: The treatment of $[Ru(\eta^6\text{-}p\text{-cymene})Cl_2]_2$ with N,N'-(1,2-phenylene)dipicolinamide (**H₂L1**) afforded the double salt complex $[\{Ru(\eta^6\text{-}p\text{-cymene})_2\text{-}\mu\text{-Cl}\}\textbf{L1}][Ru(\eta^6\text{-}p\text{-cymene})Cl_3]$, (**Ru1**) in moderate yields. Separately, the reactions of ligands (**H₂L1**), N,N'-(4,5 dimethyl-1,2-phenylene)dipicolinamide (**H₂L2**), and N,N'-(4-methoxy-1,2-phenylene)dipicolinamide (**H₂L3**) with the $[Ru(\eta^6\text{-}p\text{-cymene})Cl_2]_2$ in the presence of KPF_6 afforded the respective dinuclear half-sandwich Ru(II) complexes $[\{(Ru(\eta^6\text{-}p\text{-cymene})_2\text{-}\mu\text{-Cl}\}\textbf{L1}][PF_6]$ (**Ru2**), $[\{(Ru(\eta^6\text{-}p\text{-cymene})_2\text{-}\mu\text{-Cl}\}\textbf{L2}][PF_6]$ (**Ru3**), and $[\{(Ru(\eta^6\text{-}p\text{-cymene})_2\text{-}\mu\text{-Cl}\}\textbf{L3}][PF_6]$ (**Ru4**). NMR and FT-IR spectroscopies, ESI-MS spectrometry, and elemental analyses were used to establish the molecular structures of the new dinuclear ruthenium(II) complexes. Single crystal X-ray crystallography was used to confirm the piano-stool geometry of the dinuclear complexes **Ru1** and **Ru4**, as containing N^N chelated ligand and bridging *chlorido* ligands in each Ru(II) atom. The complexes (**Ru1-Ru4**) showed good catalytic activities at low catalyst concentrations of 0.005 mol% in the transfer hydrogenation of a wide range of ketone substrates.

Keywords: carboxamide; ruthenium(II); structures; transfer hydrogenation; ketones

1. Introduction

Transition metal catalysed transfer hydrogenation (TH) reactions have provided a versatile and efficient protocol for the syntheses of valuable bulk and fine chemicals [1,2]. Ever since the first (S)-BINAP/diamine-Ru(II) complexes were employed as catalysts in the transfer hydrogenation (TH) of ketones by Noyori and Ikariya [3], a plethora of transition-metal-based catalysts have been developed for transfer hydrogenation reactions [4,5]. While a number of mononuclear-metal-based complexes have been shown to give promising catalytic activities in the TH of, for example, ketones, the use of multinuclear analogues is still in its infancy [6]. Thus, the development of multinuclear complexes to mediate these TH reactions is beginning to grain traction with the aim of enhancing catalytic activity and stability [7–9]. Few examples of multinuclear complexes based on Ru(II) [5,7], Ir(I/III) [10–12], and Rh(II) [13] metals have so far been reported in the TH of ketones. Many of these complexes are derived from *N*-heterocarbene (NHCs) [11], Schiff bases [14], and phosphinite–Schiff base ligands [15].

In the design of multinuclear catalysts, key factors such as the electronic property and adaptability of a chelating ligand are considered [15]. For example, a ligand framework bearing multi-donor sites often favours the stabilisation of polynuclear complexes [16,17]. Another versatile method of synthesising multinuclear complexes is the one-pot coordination of polydentate ligands by a metal salt. This strategy is essentially viable in terms of the atom economy, the yield, the compatibility of the metal centres and coordination sites, and the ease of coordination between the metal atom and the ligand framework [17].

Following these synthetic protocols, a number of polynuclear complexes anchored on N^N^N donor ligands have been developed and shown to give promising catalytic

activities in TH reactions [7,8,18]. In one such approach, a dinuclear Ru(II)-NˆNˆN complex, bearing a 4,4′-(CH$_2$)$_3$-bipyridine linker, was reported to give high catalytic activity (TOF up to 1.4×10^7 h^{-1}) towards the TH of ketones [7]. Recently, tri- and hexanuclear ruthenium(II) complexes obtained by assembling 16-e$^-$ Ru(II) pyrazolyl-imidazolyl- units with polypyridines, also display TOFs up to 7.1×10^6 h^{-1} in the TH of ketones [7]. Having been encouraged by our earlier findings on the synthesis and applications of mononuclear carboxamide Ru(II) complexes in the TH of ketones [19], herein, we report the synthesis, structural elucidation, and applications of symmetrical dinuclear piano-stool ruthenium(II)-dipicolinamide complexes as catalysts in the TH of ketones.

2. Results and Discussion

2.1. Synthesis and Characterisation of Ligands and Complexes

The multifunctional (pyridyl)carboxamide ligands, *N*,*N*′-(1,2-phenylene)dipicolinamide (**H$_2$L1**), *N*,*N*′-(4-methoxy-1,2-phenylene)dipicolinamide (**H$_2$L2**), and *N*,*N*′-(4,5 dimethyl-1,2-phenylene)dipicolinamide (**H$_2$L3**) were synthesised following a modified procedure from the literature [20–24]. The synthetic details and spectroscopic data of the dicarboxamide ligands are given as supplementary data, **ESI†**. The treatment of the [Ru(η^6-*p*-cymene)Cl$_2$]$_2$ precursor with the dipicolamide ligand **H$_2$L1** in the presence of sodium methoxide (NaOMe) resulted in the formation of the dinuclear Ru(II) complex [{Ru(η^6-*p*-cymene)$_2$-*μ*-Cl}**L1**][Ru(η^6-*p*-cymene)Cl$_3$] (**Ru1**), as illustrated in Scheme 1. The reactions of the [RuCl$_2$(η^6-*p*-cymene)]$_2$ precursor with the ligands **H$_2$L1**, **H$_2$L2**, and **H$_2$L3** in the presence of KPF$_6$ gave the cationic complexes [{(Ru(η^6-*p*-cymene)$_2$-*μ*-Cl}**L1**][PF$_6$] (**Ru2**), [{(Ru(η^6-*p*-cymene)$_2$-*μ*-Cl}**L2**][PF$_6$] (**Ru3**), and [{(Ru(η^6-*p*-cymene)$_2$-*μ*-Cl}**L3**][PF$_6$] (**Ru4**), respectively (Scheme 1).

All the isolated complexes were characterised using NMR spectroscopy, mass spectrometry, FT-IR spectroscopy, microanalysis, and single-crystal X-ray crystallography (**Ru1** and **Ru3**). The formation of the dinuclear Ru(II) complexes **Ru1**–**Ru4** was confirmed by comparing their ^{1}H NMR spectroscopic data to their corresponding free ligands **H$_2$L1**–**H$_2$L3** (Figures S1–S7). For instance, in the ^{1}H NMR spectrum ligand **H$_2$L1**, the signal assigned to the amide proton (N-H) observed at δ: 10.17 ppm disappeared upon coordination to form the corresponding complex **Ru2** (Figure S1 vs. Figure S5). Similar ^{1}H NMR spectral data were observed for the other complexes **Ru1, Ru3,** and **Ru4** (Figures S1–S7, ESI†). This was an indicative of the deprotonation of the amide protons prior to complexation, as has been observed in other related complexes [24,25], and was consistent with the solid-state structures of complexes **Ru1** and **Ru4** (Figures 1 and 2). In addition, the ^{1}H NMR spectra of complexes **Ru1**–**Ru4** displayed signals of the pyridine protons downfield (7.80–9.40 ppm) compared to 8.69–7.45 ppm in the free ligands (**HL1**–**HL3**). ^{13}C{^{1}H} NMR spectroscopy was also useful in establishing the formation of the dinuclear Ru(II) complexes. For example, the carbonyl carbon signals in complexes **Ru1**–**Ru4** were observed downfield in comparison with the signals of the corresponding free ligands (Figures S8–S14). For instance, the ^{13}C{^{1}H} NMR spectrum of complex **Ru2** showed the carbonyl (C=O) signal downfield at 169.6 ppm (Figure S12) compared to the signal at 163.3 ppm for its free ligand **H$_2$L2** (Figure S8). This trend is reasonable, since the C=O motif is within the Ru(II) coordination sphere and is likely to be electron-deficient (ligands predominantly sigma-donors). ^{31}P{^{1}H} NMR spectra of **Ru2**–**Ru4** exhibited a septet signal between ~131 and ~157 ppm (Figures S15 and S17) and established the presence of the PF$_6$$^-$ counter-anion in these compounds, as depicted in Scheme 1. This was further supported by ^{19}F NMR spectroscopic data which displayed doublet signals in the range of −69 ppm to −71 ppm (Figures S18 and S20).
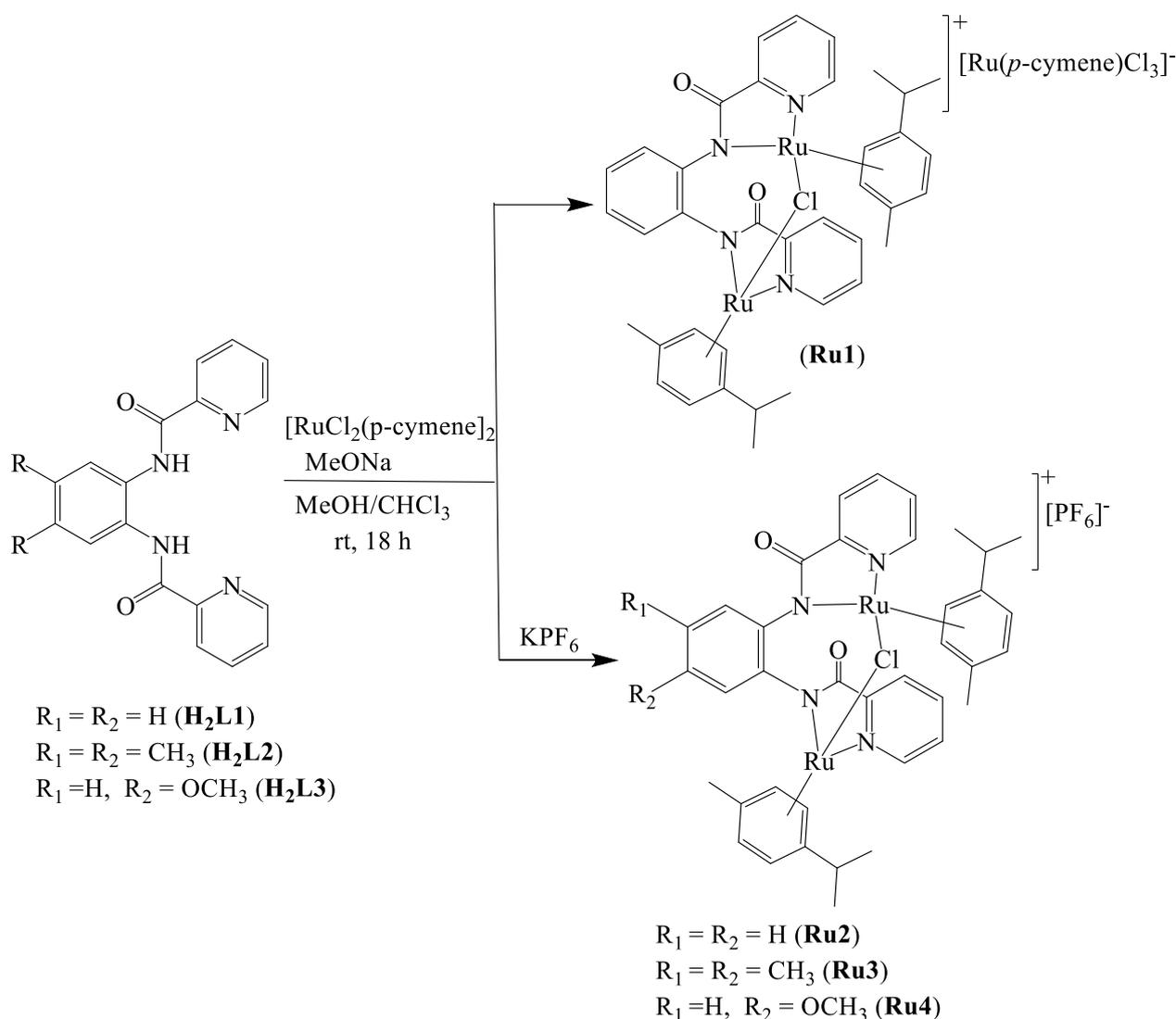
Scheme 1. Preparation of dinuclear piano-stool ruthenium(II) compounds **Ru1–Ru4**.

The successful formation of complexes **Ru1–Ru4** was further supported by comparing their FT-IR spectra to their respective free ligands **H₂L1–H₂L3** (Figures S21–S27). As noted in the ^{1}H NMR spectroscopic data, the sharp signal of the amidic N–H functional group in **H₂L2,** recorded at 3325 cm^{-1}, disappeared in the spectrum of the corresponding complex **Ru3**. Similar observations were recorded in the FT-IR spectroscopic data of the other complexes **Ru1, Ru2,** and **Ru4**. Furthermore, the FT-IR spectroscopic data of complexes **Ru1–Ru4** (Figures S24–S27) showed the (C=O) signals at lower frequencies (1618–1620 cm^{-1}) compared to their corresponding free ligands **H₂L1–H₂L3** (1664–1688 cm^{-1}). These could be assigned to the resonance enhancement within the deprotonated ligand leading to the weakening of the carbonyl (C=O) group in the coordinated ligands [22,23,26]. Mass spectrometry was also employed to elucidate the molecular compositions of complexes **Ru1–Ru4**. The compounds gave base peaks at m/z = 825 (**Ru1** and **Ru2**), 853 (**Ru3**), and 851(**Ru4**), corresponding to the parent cations [M]$^+$, signifying the stability of the compounds. In addition, the experimental isotopic mass distributions correlated well with the theoretical patterns (Figures S31–S34, ESI†). The elemental analyses data of the complexes tallied well with the proposed empirical formulae, as shown in Scheme 1.
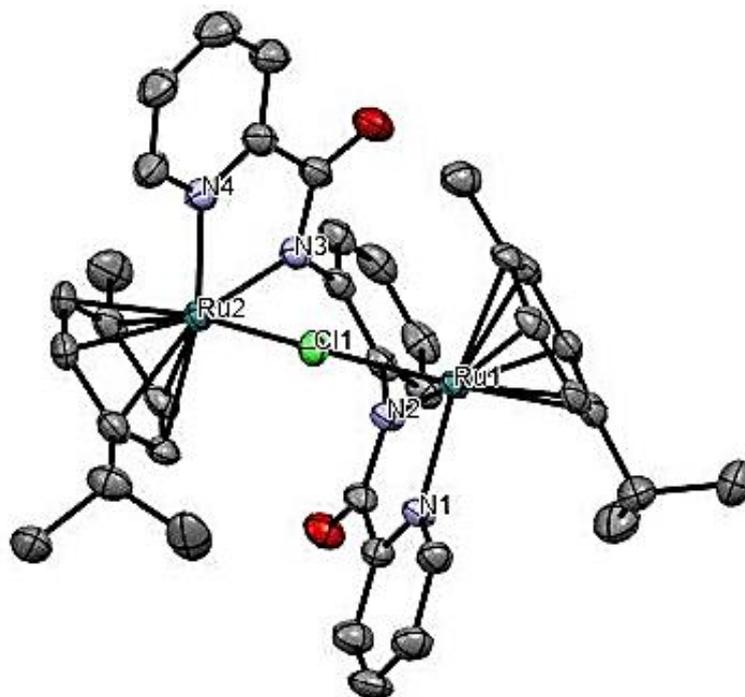
Figure 1. Molecular structure of **Ru1,** with ellipsoids drawn at 50% probability level. Hydrogen atoms, CH_2Cl_2 solvent and $[RuCl_3(\text{p-cymene})]^-$ counter-anion have been omitted for clarity. Selected bond lengths (Å): N(1)-Ru(1), 2.104(4); N(2)-Ru(1), 2.094(4); Ru(1)-Cl(1), 2.4526(12); Ru(1)-Ru(2), 4.168(5). Selected bond angles (°): N(1)-Ru(1)-N(2), 77.55(15); N(1)-Ru(1)-Cl(1), 85.37(11); N(2)-Ru(1)-Cl(1), 86.96(11); Ru(1)-Cl(1)-Ru(2), 115.68(4).
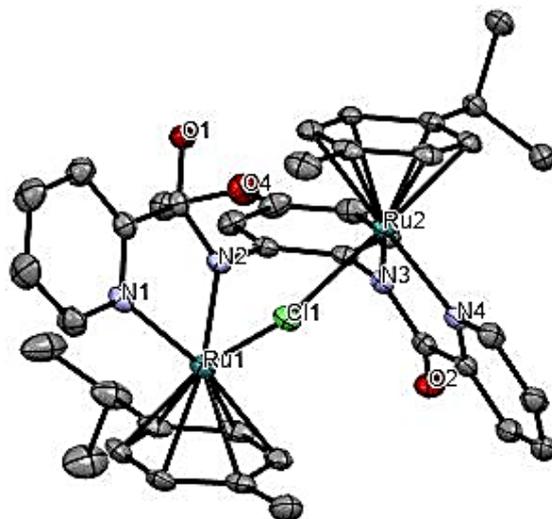
Figure 2. Molecular structure of **Ru4**, with ellipsoids drawn at 50% probability level. Hydrogen atoms and $[PF_6]^-$ counter-anion are omitted for clarity. Selected bond distances (Å): N(1)-Ru(1), 2.097(2); N(2)-Ru(1), 2.081(2); Ru(1)-Cl(1), 2.4627(7); Ru(1)-Ru(2), 4.168(5). Selected bond angles (°): N(2)-Ru(1)-N(1), 77.54(9); N(1)-Ru(1)-Cl(1), 83.23(7); N(2)-Ru-Cl(1), 85.79(6).

2.2. Molecular Structures of Ruthenium(II) Complexes Ru1 and Ru3

The slow diffusion of diethyl ether into dichloromethane solutions of complexes **Ru1** and **Ru4** gave single crystals suitable for X-ray analyses. Figures 1 and 2 show the molecular structure of the cationic complexes **Ru1** and **Ru4**, respectively, while the crystallographic data are shown in Table 1. The packing diagrams and structures of the compouds showing the counter anions and solvent molecules are given in Figures S35–S38. Complexes **Ru1** and **Ru4** crystallise in triclinic and monoclinic systems with P-1 and P2$_1$/c, space groups,

respectively. The net charge on the cationic species in **Ru1** and **Ru4** are balanced by the counter-anions $[Ru(\eta^6\text{-}p\text{-cymene})Cl_3]^-$ and $[PF_6]^-$, respectively. The half-sandwich complexes **Ru1** and **Ru4** exhibit three-legged piano stool geometry (Figures 1 and 2), which is typical of $[Ru(\eta^6\text{-}p\text{-cymene})(\mathbf{L})Cl]^+$ complexes. In the coordination sphere of both compounds, **Ru1** and **Ru4**, the *p*-cymene ring resides on the apex, whereas the bridging *chlorido* ligands, $N_{pyridine}$ ˆ and $N_{amidate}$ chelate, constitute the base of the piano stool. In the two complexes (**Ru1** and **Ru4**), the five-membered chelating rings have an average bite angle for $N_{pyridine}$ -Ru- $N_{amidate}$ of 77.18 (18)° Å. The two Ru(II) atom centres in both compounds are separated by an average distance of 4.167 (5) Å, which is relatively shorter than the average 5.613 ± 18 Å calculated for 9 half-sandwich dinuclear ruthenium(II) complexes [27]. The average bond distance for Ru-$N_{pyridine}$ and Ru-$N_{amidate}$ of 2.093 (2) Å and 2.109 (2) Å in compounds **Ru1** and **Ru4** are within the mean bond length for Ru-$N_{pyridine}$ = 2.090 (14) Å and Ru-$N_{amidate}$ of 2.083 (22) Å, obtained from three (3) piano-stool Ru(II) complexes [27]. The *p*-cymene rings in the compounds are almost planar, with the Ru(II) atoms at 3.205(11) Å distance from the centroid of the *p*-cymene rings, and are comparable to the average 3.182(18) Å calculated for 18 half-sandwich Ru(II) structures [27].

Table 1. Summary of crystallographic parameters and refinement data.

Parameters	Ru1	Ru4
Empirical formula	$C_{48}H_{54}Cl_4N_4O_2Ru_3+[CH_2Cl_2]$	$C_{39}H_{42}ClF_6N_4O_3PRu_2$
Formula weight	1418.74	997.32
Temperature/K	100 (2)	100 (2)
Wavelength(Å)	1.54178	1.54170
Crystal system	Triclinic	Monoclinic
Space group	P-1	$P2_1/c$
Unit cell dimensions;		
a	13.121 (2)Å	15.3868 (4)
b	15.820 (3)Å	19.3230 (5)
c	16.506 (4)Å	13.7638 (4)
α	61.430 (6)○	90
β	71.530 (11)○	101.771 (1)
γ	72.142 (7)○	90
Volume	2803.9 (10)Å^3	4006.18 (19)
Z	2	4
Density (calculated) / Mg/m^3	1.680	1.654
Absorption coefficient/ mm^{-1}	11.186	7.713
F(000)	1424.0	200080
Crystal Size (mm^3)	0.14 × 0.095 × 0.07	0.15 × 0.15 × 0.15
Theta range for data collection	71.961	68.225
Reflections collected	11036	7297
Completeness	97.6%	99.4%
Refinement method	Full-matrix least-square on F^2	Full-matrix least-square on F^2
Goodness-of-fit on F^2	1.076	1.057
Final R indices [I>2sigma(I)]	R$_1$ = 0.0511, wR$_2$ = 0.1447	R$_1$ = 0.0278, wR$_2$ = 0.0782
R indices (all data)	R$_1$ = 0.0567, wR$_2$ = 0.1509	R$_1$ = 0.0282, wR$_2$ = 0.0785
Largest diff. peak and hole/eA^{-3}	1.55/−2.57	1.42/−0.50

2.3. Transfer Hydrogenation of Ketones

To explore the feasibility of the dinuclear Ru(II) compounds (**Ru1–Ru4**) to mediate the TH of ketones, acetophenone (1.12 mL, 1.00 mmol) and K^{t}BuO (0.4 mol%) were used as model substrate and base, respectively (Table 2). ESI Figures S39–S46 show the ^{1}H NMR spectral data of the crude TH mixtures used to determine the respective percentage conversions and yields with time. In the presence of K^{t}BuO (1.00 mL of 0.04 M in 2-propanol), complex **Ru2** (5.5×10^{-4} mol%, 550 ppm) achieved percentage yields of 98% corresponding to a TOF of 2.2×10^2 h^{-1} in the TH of acetophenone in 6 h (Table 2, entry 7). To succinctly verify the role played by complex **Ru2** and the K^{t}BuO base, we carried out some control experiments. Firstly, a Ru-catalyst-free experiment employing only the K^{t}BuO base was performed, and afforded negligible percentage yields of 1% within 6 h (Table 2, entry 1), consistent with the findings of Tenorio and co-workers [28]. In another set of

control experiments, a base-free reaction gave lower percentage yields of 30% in 6 h (Table 2, entry 2). From these control results, it is therefore plausible to assign the higher percentage yields to the ruthenium(II) complexes in these TH reactions.

Table 2. Effects of catalyst concentration and base on transfer hydrogenation of acetophenone using complex **Ru2** as a catalyst [a].
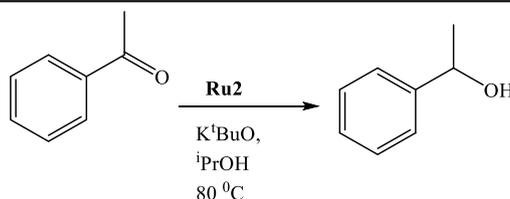
Entry	Catalyst Loading/$\times 10^{-3}$ mol% (ppm)	Base	[b] Conversion[%]	Yield%	TON $\times 10^4$	TOF $\times 10^3$/h^{-1}
1	-	K^{t}BuO	2	1	-	-
2	5.00 (50)	-	32	30	0.64	1.07
3	2.50 (25)	K^{t}BuO	41	39	1.56	2.60
4	5.00 (50)	K^{t}BuO	86	85	1.72	2.87
5	15.00 (150)	K^{t}BuO	95	94	0.63	1.05
6	25.00 (250)	K^{t}BuO	96	95	0.26	0.43
7	55.00 (550)	K^{t}BuO	99	98	0.13	0.22
8	5.00 (50)	KOH	76	76	1.71	2.85
9	5.00 (50)	K$_2$CO$_3$	29	28	0.58	0.97

[a] Conditions: 1.0 mmol acetophenone, 0.4 mol%, ^{t}BuOK in 1.00 mL ^{i}PrOH, temperature 80 °C, time = 6 h. [b] Determined by ^{1}H NMR spectroscopy. Anisole was used as an internal standard. Turnover number (TON) = moles of product formed/moles of catalyst used. Turnover frequency (TOF) = moles of product formed/moles of catalyst/time (h). Experiments were performed in triplicate to ensure reproducibility (standard deviation, S.D = ±1.0).

Having established the viability of complex **Ru2** to mediate the catalytic transfer of acetophenone, we then studied the effect of catalyst concentration by varying the catalyst loadings from 0.0025 to 0.055 mol% (Table 2, entries 3–7). From the results, while a general increase in catalyst loading resulted in higher percentage yields, lower catalytic activities (TOFs and TONs) were observed (Figure S47). For instance, an increase in the catalyst loading, from 0.0025 to 0.055 mol%, was accompanied by an increase in the percentage yields, from 39% to 98%, but a decrease in TOF from 2.60×10^3 h^{-1} to 2.2×10^2 h^{-1} (Table 2, entries 3 vs. 7); this is in line with the previous reports of Yu and co-workers, and has been attributed to the lower magnitudes of catalytic activities at higher catalyst loadings [7]. The nature of the base is known to greatly influence the performance of the metal catalysts in the TH of ketones. Thus using catalyst **Ru2**, we tested the various bases K$_2$CO$_3$ and KOH, and established the order of catalytic activity as K$_2$CO$_3$ < KOH < ^{t}BuOK (Table 2, entry 4, 8 and 9), consistent with the relative strengths of the bases [9].

2.3.1. Influence of Catalyst Structure on the TH of Acetophenone

Having established the optimised reaction parameters (catalyst loading, 5.00×10^{-3} mol% (50 ppm); ^{t}BuOK, 4.0 mol% and temperature, 82 °C), we sought to investigate the effects of the catalyst structure/ligand motif on the transfer hydrogenation of ketones. In general, all the pre-catalysts showed appreciable catalytic activities (TOFs between 1.72×10^3 h^{-1} and 1.97×10^3 h^{-1}), comparable to the phosphine–amide ruthenium(II) complexes reported in the literature [20]. As demonstrated in Figure 3 and Figure S48 and Table 3, complexes **Ru3** and **Ru4**, bearing methyl and methoxy electron-donating groups on the phenyl linker, exhibited slightly higher catalytic activities compared to the unsubstituted analogue **Ru2** (Table 3, entries 2–4). For example, complex **Ru3** (methyl) displayed a TOF of 3.13×10^3 h^{-1} ($k_{obs} = 1.73 \times 10^{-1} \pm 0.12$) compared to the TOF of 2.87×10^3 h^{-1} (k_{obs} of 1.69×10^{-1} (±0.03) h^{-1}) recorded for the unsubstituted **Ru2**, (Table 3, entries 3 vs. 4). While electron-donating groups are expected to result in lower catalytic activity due to the diminished electrophilicity of the metal centre, the higher catalytic activities of complexes **Ru3** and **Ru4** could be assigned to the improved stability of the resultant active species [29–31]. Interestingly, complex **Ru1** gave the highest catalytic activity, which may be ascribed

to the presence of the [Ru(*p*-cymene)Cl$_3$]$^-$ counter-anion, which, on its own, could act as a catalyst (double catalyst) in the TH of acetophenone (Table 3, entry 1).
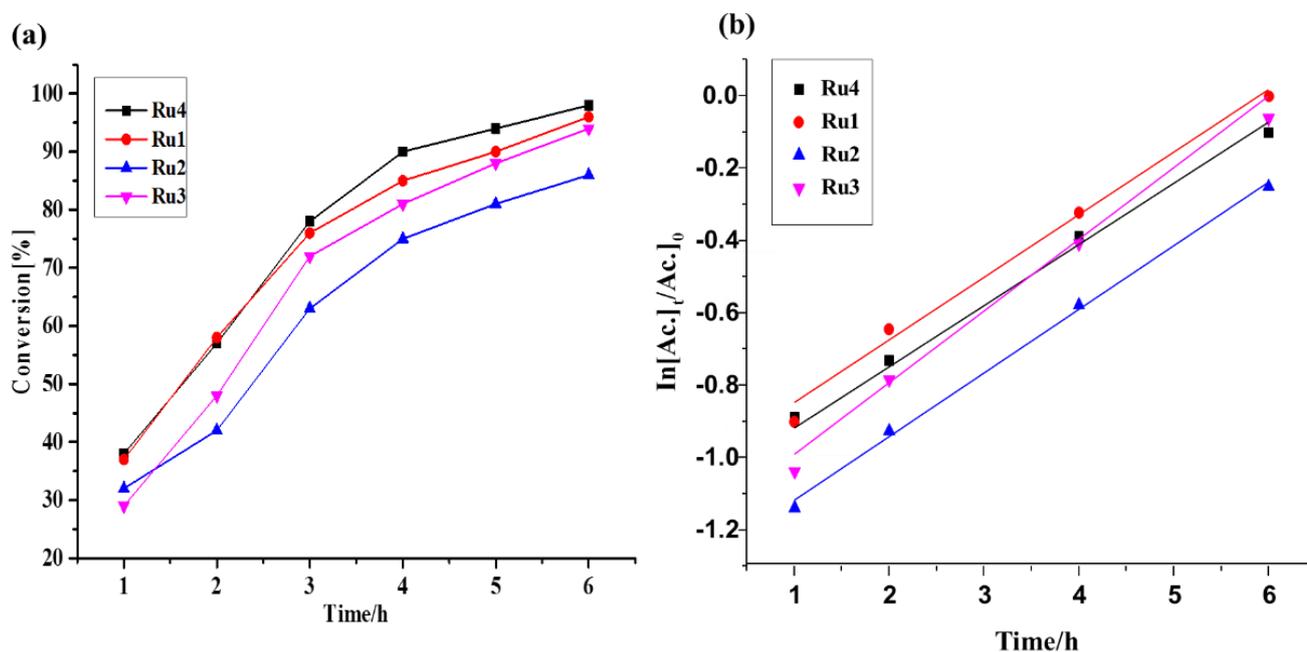
Figure 3. Time-dependent transfer hydrogenation reaction of acetophenone catalysed by **Ru1**–**Ru4**, 5.00×10^{-3} mol% (50 ppm); ^{t}BuOK: 4.0 mol%; temp. 82 °C). (**a**) Yield (%) vs. time graph, (**b**) $-\ln[\text{Ac.}]_t/[\text{Ac.}]_0$ vs. time plot of the **Ru1**–**Ru4** catalysts (Ac.—acetophenone).

Table 3. Transfer hydrogenation of acetophenone catalysed by **Ru1**–**Ru4** complexes: Effect of catalyst structure [a].

Entry	Catalyst	[b] Conv. [%]	[b] Yield [%]	TON $\times 10^4$	TOF/h^{-1} x 10^3	$k_{obs} \times 10^{-1}$/h^{-1}
1	[RuCl$_2$(*p*-cymene)$_2$]	12	11	0.02	0.03	–
2	**Ru1**	99	98	1.96	3.27	1.97
3	**Ru2**	86	85	1.72	2.87	1.69
4	**Ru3**	96	94	1.88	3.13	1.76
5	**Ru4**	92	92	1.84	3.07	1.73

[a] Conditions: acetophenone: 1.00 mmol; [**Ru**]: 5.00×10^{-3} mol% (50 ppm); ^{t}BuOK: 4.00 mol% in 2.5 mL and diluted with 1.00 mL ^{I}PrOH, temperature 80 °C, 6 h. [b] Determined by ^{1}H NMR spectroscopy. Anisole was used as an internal standard. [c] [Ru] = 5.5×10^{-2} mol% (550 ppm). Turnover number (TON) = moles of product formed/moles of catalyst, [**Ru**] = concentration of the catalyst. Turnover frequency (TOF) = moles of product formed/moles of catalyst/time (h), [**Ru**] = concentration of the catalyst. Experiments were performed in triplicate to ensure reproducibility, S.D = ±1.0).

The catalytic activities of complexes **Ru1**–**Ru4** (TOF of up to 3.27×10^3 h^{-1}) compared poorly with some of the highly active multinuclear Ru(II)-based catalysts which demonstrated TOFs up to 1.0×10^6 h^{-1}, as reported in the literature [7,9,18]. While the carboxamide ligands have the propensity to stabilise the Ru(II) complexes, the relatively lower catalytic activities observed for complexes **Ru1**–**Ru4** could be linked to the larger internuclear distance between the two metal centres, thus hindering the mutual interactions between the two metal centres [30,31]. On a positive note, the complexes showed higher catalytic activities compared to reported half-sandwich nitrogen-donor ruthenium(II) complexes, where TOFs of 5×10^2 h^{-1} were recorded [5,32–36].

2.3.2. Investigation of the Ketone Substrate Scope

To study the applicability of the catalysts in the TH of a wide range of ketones, catalysts including heteroaromatic and aliphatic ketones were investigated using complex **Ru2** (Table 4). From the Table 4, acetophenone derivatives containing electron-withdrawing substituents displayed higher percentage yields. For example, 2-chloroacetophenone and 4-chloroacetophenone furnished a percentage yield of 99% in 4 h compared to acetophenone, which attained 86% in 6 h (Table 4, entries 1 vs. 2 and 3). This observation could be explained by the reduction in electron density on the carbonyl carbon, thus facilitating nucleophilic attack [9,37]. In sharp contrast, the introduction of electron-donating groups led to diminished catalytic activities of complex **Ru2**. As an illustration, 4-amino acetophenone exhibited lower percentage yields of 78% compared to that of acetophenone, at 86% (Table 4, entries 1 vs. 9). The trend of reactivity of the substrates were not significantly affected by the position of the electron-donating groups on the phenyl ring. For instance, 2-methyl acetophenone and 4-methyl acetophenone exhibited comparable percentage yields of 81 and 79% (Table 4, entries 5 vs. 6). This trend points to electronic factors in the substrates playing a key role in controlling the catalytic activities of complex **Ru2**. With steric effect, 2-methyl acetophenone (more sterically demanding) would be expected to give lower percentage yields than 4-methyl acetophenone. Indeed, this hypothesis was augmented by the lower percentage yields of 79% (6 h) reported for 4-methyl acetophenone compared to percentage yields of 99% (4 h) recorded for of 4-chloroacetophenone (Table 4, entries 3 and 6). Similar trends were previously reported by Chai et al., using dinuclear ruthenium(II) complexes supported on tridentate nitrogen-donor ligands [9].

Table 4. Investigation of substrate scope using complex **Ru2** as a catalyst [a].

Entry	Ketone	[b] Yield (%)	Entry	Ketone	[b] Yield%
1		86	8		75
2 *		99	9		78
3 *		99	10		88
4		70	11		84
5		81	12		76
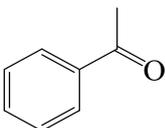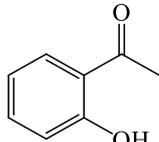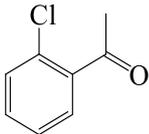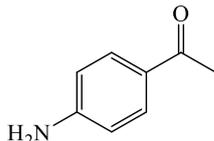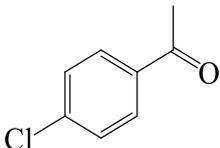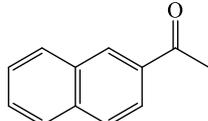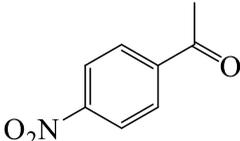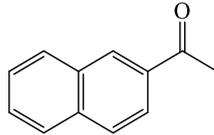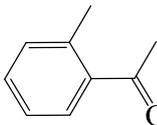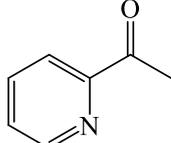
Table 4. *Cont.*

Entry	Ketone	[b] Yield (%)	Entry	Ketone	[b] Yield%
6		79	13		73
7		78	14		88
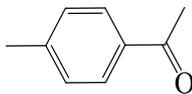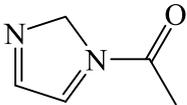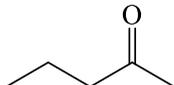
[a] Conditions: 1.0 mmol acetophenone, *t*BuOK (4.00 mol%) in 2.5 mL and diluted with 1.00 mL *i*PrOH, **Ru2,** 5.00×10^{-3} mol% (50 ppm) temperature 80 °C, 6 h. [b] Determined by ^{1}H NMR spectroscopy. Anisole was used as an internal standard. * Reaction time = 4 h. (All experiments were carried outs in triplicate to ensure reproducibility, S.D = ±1.0).

Acetophenone derivatives containing polyaromatic groups such as 2-acetylnaphthalene also realised decent percentage yields of 88% comparable to yields of 86% recorded for acetophenone (Table 4, entries 1 vs. 10, 11) which are in line with the findings of Chai et al. [9]. More significantly, heteroaromatic acetophenone derivatives such as 1-acetyl imidazole also afforded moderate percentage yields of 76% (Table 4, entries 12, 13). The relatively lower yields realised for 1-acetyl imidazole compared to acetophenone (86%) could be assigned to the irreversible binding of the N-donor atoms of the hetero-atoms of the substrates to the active Ru(II) centre [7]. Interestingly, and contrary to the known trends, aliphatic ketones such as 2-pentanone were also reduced with comparable percentage yields of 88% to acetophenone of 86% (Table 4, entries 1 vs. 14). In an earlier report by Liu et al. [7], aliphatic ketones showed lower catalytic activities compared to acetophenone [38]. The reasons for this behaviour of complex **Ru2** (higher catalytic activities for aliphatic ketones) is still not clear to us at this stage.

3. Conclusions

In conclusion, four cationic dinuclear Ru(II) complexes ligated on carboxamide ligands have been structurally characterised and studied as pre-catalysts in the TH of ketones. The ruthenium complexes (**Ru1** and **Ru4**) exhibit three-legged piano stool geometry around their Ru(II) atoms, in which the coordination sphere consists of N^O chelate, one bridging *chlorido*, and η⁶-*p*-cymene ligands. The Ru(II) compounds formed active catalysts in the TH of ketone substrates, giving moderate to high catalytic activities of TONs of up to 1.96×10^3 at very low catalyst concentrations. The complexes bearing electron-donating groups (**Ru3** and **Ru4**) on the ligand backbone were more active than their unsubstituted counterparts (**Ru2**). Additionally, ketone substrates containing electron-donating groups and heteroatoms afforded lower percentage yields when compared to substrates bearing electron-withdrawing groups. Thus, the stability of the complexes and the nature of the electronic properties of the ketone substrates appeared to regulate the catalytic performances of these complexes in the TH.

4. Experimental Section

4.1. Materials and Instrumentations

All synthetic manipulations, unless otherwise stated, were carried out using the standard Schlenk technique under an inert atmosphere. All solvents were distilled and dried according to standard purification procedures [39]. Starting materials, 2-picolinic acid, *p*-phenylenediamine, *o*-phenylenediamine, 4-methoxy benzene-1,2-diamine, 4,5-diamethylbenzene-1,2-diamine, triphenylphosphate, sodium methoxide and [Ru(η⁶-*p*-cymene)Cl₂]₂ precursors were purchased from Sigma Aldrich and used without further purification. The carboxamide ligands, *N, N'*-(1,2-phenylene)dipicolinamide (**H₂L2**), *N, N'*-(4,5-dimethyl-1,2-phenylene)dipicolinamide (**H₂L2**), and *N, N'*-(4-methoxy-1,2-phenylene)-dipicolinamide (**H₂L3**) were prepared following the literature procedure [21–24], and Nu-

clear Magnetic Resonance (NMR) spectra were acquired on a Bruker Avance Ultrashield 400 MHz spectrometer using *d*-CDCl$_3$ and *d*$_6$-DMSO as solvents at room temperature. The chemical shift values of ^{1}H, ^{13}C{^{1}H}, ^{19}F and ^{31}P{^{1}H} NMR are recorded in parts per million (ppm) relative to TMS with the residual solvent peak as an internal reference and coupling constants are measured in Hertz (Hz) [40]. Mass spectrometry and elemental analyses were performed on a micro-mass LCT premier mass spectrometer and Flash 2000 Thermo scientific analyser, respectively.

4.2. X-ray Data Collection, Structure, and Refinement

A single crystal suitable for X-ray diffraction analysis was mounted on a glass fibre with epoxy cement. The crystals have been cut to size (less than collimator cross-section diameter). The X-ray data of the complexes were collected on the Bruker Apex-II CCD at 100 K and the graphite monochrome Cu-Kα radiation at 0.71073 Å. Structures were initially resolved by direct method programs (SIR-92) and further refined by the full-matrix least-squares techniques on F^2 using SHELXL-2015 [41]; all calculations were manipulated using the WinGX-2018 crystallographic package. A SADABS semi-empirical multi-scan absorption correction was applied to the data. Direct methods, SHELXS-2015 and WinGX-2018, were used to solve the structure. All non-hydrogen atoms were located in the difference density map and refined anisotropically with SHELX-2015. All hydrogen atoms were included as idealised contributors in the least-squares process. The positions of all hydrogen atoms were calculated using a standard riding model with C–H$_{aromatic}$ distances of 0.93 Å and U$_{iso}$ = 1.2 U$_{eq}$ and CH$_{methylene}$ distances of 0.99 Å and U$_{iso}$ = 1.2 U$_{eq}$ and C–H$_{methyl}$ distances of 0.98 Å and U$_{iso}$ = 1.5 Ueq.

4.3. Synthesis of Dinuclear Ruthenium(II) Carboxamide Complexes

4.3.1. [{Ru(η^6-p-cymene)$_2$-μ-Cl}$_2$**L1**][Ru(η^6-p-cymene)Cl$_3$] (**Ru1**)

To a solution of dichloro-ruthenium *p*-cymene dimer, [Ru(η^6-*p*-cymene)Cl$_2$]$_2$ (0.10 g, 0.16 mmol) in the mixed methanol and chloroform (1/1, 10/10 mL), **H$_2$L1** (0.06 g, 0.16 mmol) and sodium methoxide, NaOMe (0.02 g, 0.32 mmol) were added, and the resultant mixture was reacted at 25 °C for 18 h. The resultant orange suspension was evaporated, and the crude product was dissolved in dichloromethane and filtered over celite. The filtrate was then concentrated to about 3 mL, diethyl ether (20 mL) was added, and the mixture filtered and dried in vacuum to obtain an orange compound. Yield: 0.16 g (86%). ^{1}H NMR (400 MHz, CDCl$_3$) δ: 9.40 (d, $^3J_{HH}$ = 5.6, 2H$_{pyridine}$), 8.28(t, $^3J_{HH}$ = 7.6, 2H$_{pyrdine}$), 8.11(d, $^3J_{HH}$ = 7.6, 2H$_{pyridine}$), 7.88(t, $^3J_{HH}$ = 8.0, 2H$_{pyridine}$), 7.56(dd, $^3J_{HH}$ = 3.6, 2H$_{benzene}$), 7.27(dd, $^3J_{HH}$ = 3.6, 2H$_{benzene}$), 5.62(d, $^3J_{HH}$ = 4.4 Hz, 2H$_{pcymene}$), 5.52(d, $^3J_{HH}$ = 4.4 Hz, 2H$_{pcymene}$), 5.30(d, $^3J_{HH}$ = 4.4 Hz, 2H$_{pcymene}$), 5.05(d, $^3J_{HH}$ = 4.4 Hz, 2H$_{pcymene}$), 2.12(m, $^3J_{HH}$ = 6.8 Hz, 2H$_{pcymene}$), 1.19 (s, 6-H$_{pcymene}$), 0.98 (d, $^3J_{HH}$ = 6.8 Hz, 6H$_{pcymene}$), 0.81 (d, $^3J_{HH}$ = 6.8, 6H$_{pcymene}$). ^{13}C{^{1}H} NMR (101 MHz, CDCl$_3$) δ:162.8, 154.1, 143.7, 139.2, 130.1, 128.9, 125.8, 124.9, 89.1, 81.4, 30.6, 22.1, 18.5. ESI-MS (*m*/*z*) at 852[M$^+$, 100%]. HR-MS (ESI): *m*/*z* 823.0958 [M$^+$], calcd for C$_{38}$H$_{40}$N$_4$O$_2$ClO$_2$Ru$_2$ 823.0927. FT-IR (cm^{-1}): ($\nu_{C=O}$)$_{amidate}$ = 1617.97; Anal. Calcd for C$_{48}$H$_{54}$Cl$_4$N$_4$O$_2$ClRu$_3$: C, 49.53; H, 4.68; N, 4.81. Found: C, 49.33.; H, 4.71; N, 4.57.

4.3.2. [{Ru(η^6-p-cymene)$_2$-μ-Cl}$_2$**L1**][PF$_6$] (**Ru2**)

To [Ru(η^6-*p*-cymene)Cl$_2$]$_2$ (0.10 g, 0.16 mmol) in a methanol and chloroform solvent system (1/1, 10/10 mL), **H$_2$L1** (0.06 g, 0.16mmol) and sodium methoxide, NaOMe (0.01 g, 0.32 mmol) were added, and reacted at room temperature for 12 h. KPF$_6$ (0.03 g, 0.16 mmol) was added, and the solution was stirred for 6 h. The resultant orange suspension was evaporated, and the crude substance was dissolved in dichloromethane and filtered over celite. The filtrate was then concentrated to about 3 mL, diethyl ether (20 mL) was added, and it was filtered and then dried in vacuum. An orange compound was obtained. Yield: 0.14 g (88%). ^{1}H NMR (400 MHz, CDCl$_3$) δ: 9.40 (d, $^3J_{HH}$ = 5.6, 2H$_{pyridine}$), 8.28(t, $^3J_{HH}$ = 7.6, 2H$_{pyrdine}$), 8.11(d, $^3J_{HH}$ = 7.6, 2H$_{pyridine}$), 7.87(t, $^3J_{HH}$ = 8.0, 2H$_{pyridine}$), 7.56(dd,

$^3J_{HH}$ = 3.6, 2H$_{benzene}$), 7.26(dd, $^3J_{HH}$ = 3.6, 2H$_{benzene}$), 5.61(d, $^3J_{HH}$ = 4.4 Hz, 2H$_{pcymene}$), 5.52(d, $^3J_{HH}$ = 4.4 Hz, 2H$_{pcymene}$), 5.34(d, $^3J_{HH}$ = 4.4 Hz, 2H$_{pcymene}$), 5.05(d, $^3J_{HH}$ = 4.4 Hz, 2H$_{pcymene}$), 2.12(m, $^3J_{HH}$ = 6.8 Hz, 2H$_{pcymene}$), 1.49 (s, 6-H$_{pcymene}$), 0.98(d, $^3J_{HH}$ = 6.8, 6H$_{pcymene}$), 0.80(d, $^3J_{HH}$ = 6.8, 6H$_{pcymene}$). ^{13}C{^{1}H} NMR (101 MHz, CDCl$_3$) δ:162.6, 154.1, 143.7, 139.2, 130.2, 128.9, 125.8, 124.9, 81.6, 30.6, 22.1, 18.7. ESI-MS (*m/z*); 823 [M$^+$, 100%]. HR-MS (ESI): *m/z* 823.0958 [M$^+$], calcd for C$_{38}$H$_{40}$N$_4$O$_2$ClO$_2$Ru$_2$ 823.0927. FT-IR (cm^{-1}): (ν$_{C=O}$)$_{amidate}$ = 1618.76. Anal. Cald. for C$_{38}$H$_{40}$ClN$_4$O$_2$Ru$_2$PF$_6$: C, 47.18; H, 4.17; N, 5.79. Found: C, 47.31; H, 3.94; N, 5.42.

4.3.3. [{Ru(η^6-p-cymene)$_2$-μ-Cl}$_2$**L2**][PF$_6$] (**Ru3**)

[Ru(η^6-*p*-cymene)Cl$_2$]$_2$ (0.10 g, 0.16 mmol), **H$_2$L2** (0.06 g, 0.16 mmol), NaOMe (0.02 g, 0.32 mmol) and KPF$_6$ (0.03 g, 0.16 mmol). An orange compound was obtained. Yield: 0.11 g (72%). ^{1}H NMR (400 MHz, CDCl$_3$) δ: 9.40 (d, $^3J_{HH}$ = 5.2, 2H$_{pyridine}$), 8.28(t, $^3J_{HH}$ = 7.2, 2H$_{pyrdine}$), 8.08(d, $^3J_{HH}$ = 7.6, 2H$_{pyridine}$), 7.80(t, $^3J_{HH}$ = 8.0, 2H$_{pyridine}$), 7.30(s, 2H$_{benzene}$), 5.61(d, $^3J_{HH}$ = 4.4 Hz, 2H$_{pcymene}$), 5.49(d, $^3J_{HH}$ = 4.4 Hz, 2H$_{pcymene}$), 5.38(d, $^3J_{HH}$ = 4.4 Hz, 2H$_{pcymene}$), 5.05(d, $^3J_{HH}$ = 4.4 Hz, 2H$_{pcymene}$), 2.12(m, $^3J_{HH}$ = 6.6 Hz, 2H$_{pcymene}$), 3.31 (s, CH$_3$), 2.32 (s, 6H$_{pcymene}$), 0.98(d, $^3J_{HH}$ = 6.6, 6H$_{pcymene}$), 0.80 (d, $^3J_{HH}$ = 6.6, 6H$_{pcymene}$). ^{13}C{^{1}H} NMR (101 MHz, CDCl$_3$) δ:162.5, 154.5, 141.0, 139.3, 133.3, 130.5, 129.0, 126.4, 125.9, 81.3, 36.4, 31.4, 24.1, 19.6. ESI-MS (*m/z*); 851 [M$^+$, 100%]. HR-MS (ESI): *m/z* 851.1271 [M$^+$], calcd for C$_{40}$H$_{44}$ClN$_4$O$_2$Ru$_2$ 81.1240. FT-IR (cm^{-1}): (ν$_{C=O}$)$_{amidate}$ = 1619.97. Anal. Cald. for C$_{40}$H$_{44}$ClN$_4$O$_2$Ru$_2$PF$_6$: C, 48.27; H, 4.46; N, 5.63. Found: C, 48.28; H, 4.42; N, 5.37.

4.3.4. [{Ru(η^6-p-cymene)$_2$-μ-Cl}$_2$**L3**][PF$_6$] (**Ru4**)

[Ru(η^6-*p*-cymene)Cl$_2$]$_2$ (0.10 g, 0.16 mmol), **H$_2$L3** (0.06 g, 0.16 mmol), NaOMe (0.02 g, 0.32 mmol) and KPF$_6$ (0.03 g, 0.16 mmol). Orange compound was obtained. Yield: 0.13 g (88%). ^{1}H NMR (400 MHz, CDCl$_3$) δ: 9.41 (m, 2H$_{pyridine}$), 8.26(m, 2H$_{pyrdine}$), 8.13(m, 2H$_{pyridine}$), 7.78(m, 2H$_{pyridine}$), 7.46(d, $^3J_{HH}$ = 4.6 Hz, 2H$_{benzene}$), 7.08(d, $^3J_{HH}$ = 4.6 Hz, 2H$_{benzene}$), 7.06(s, 1H$_{benzene}$), 5.61(d, $^3J_{HH}$ = 4.6Hz, 2H$_{pcymene}$), 5.49(d, $^3J_{HH}$ = 4.4 Hz, 2H$_{pcymene}$), 5.38(d, $^3J_{HH}$ = 4.4 Hz, 2H$_{pcymene}$), 5.05(d, $^3J_{HH}$ = 4.4 Hz, 2H$_{pcymene}$), 2.12(m, $^3J_{HH}$ = 6.6 Hz, 2H$_{pcymene}$), 3.31 (s, OCH$_3$), 2.32 (s, 6H$_{pcymene}$), 0.98(d, $^3J_{HH}$ = 6.6, 6H$_{pcymene}$), 0.80 (d, $^3J_{HH}$ = 6.6, 6H$_{pcymene}$). ^{13}C NMR (101 MHz, CDCl$_3$) δ: 169.5, 155.4, 141.0, 154.2, 144.8, 140.6, 137.4, 129.3, 128.4, 126.6, 115.09, 110.7, 86.8, 82.8, 81.3, 55.6, 20.7, 23.1, 20.9, 18.1. ESI-MS *m/z* (%); 823 [M$^+$, 100%]. FT-IR (cm^{-1}): (ν$_{C=O}$)$_{amidate}$ = 1619.11. Anal. Cald. for C$_{41}$H$_{46}$ClN$_4$O$_3$Ru$_2$PF$_6$: C, 48.03; H, 4.52; N, 5.46. Found: C, 48.14; H, 4.38; N, 5.81.

4.3.5. Transfer Hydrogenation of Experiments

A modified transfer hydrogenation of ketones produced was as followed: a stock solution of the ruthenium(II) complex, for example **Ru1** (0.0010 M) was prepared in 10.0 mL isopropanol. To a solution of acetophenone (1.15 mL, 1.00 mmol), K^{t}BuO (1 mL, 0.04 M in ^{i}PrOH) and **Ru1** (550 ppm) were added and diluted with 2.5 mL of pure ^{i}PrOH. The resultant solution was then refluxed at 82 °C, during which about 0.1 mL aliquot of the crude mixture was taken at regular time intervals. The percentage conversions and yields were determined using ^{1}H NMR spectroscopy by comparing the intensity of the methyl signals of acetophenone (s, δ$_H$: 2.59 ppm) to those of the 1-phenyl ethanol (d, δ$_H$: 1.49 ppm) of the crude products [42–45].

Supplementary Materials: The following supporting information can be downloaded at: https://www.mdpi.com/article/10.3390/inorganics10110190/s1, Crystallographic data are deposited with the Cambridge Crystallographic Data Centre, CCDC deposition numbers: 217198 and 217201. ESI (electronic supplementary information) contains the spectroscopic data used in this article. Figures S1–S7: ^{1}H NMR spectra data of ligands and Ru(II) complexes. Figures S8–S14: ^{13}C NMR spectra of the ligands and Ru(II) complexes. Figures S15–S17: ^{31}P NMR spectra of complexes **Ru2–Ru4**. Figures S18–S20: ^{19}F NMR spectra of complexes **Ru2–Ru4**. Figures S21–S27: FT-IR spectra of the ligands and Ru(II) complexes. Figures S28–S34: ESI-MS spectra of ligands and Ru(II)

complexes. Figures S35–S38: Molecular structures and packing diagrams of complexes **Ru1** and **Ru4**. Figures S39–S46: ^{1}H NMR spectra of TH aliquots taken at different time intervals for determination of percentage yields. Figure S47: A plot of Conversion, TOF vs catalyst loading used to determine optimised reaction conditions. Figure S48: The plot of $In[Ac.]_t/[Ac.]_0$ vs. time for determination of k_{obs} of the catalysts.

Author Contributions: R.T.K.: Investigation, experimental work, validation, software, formalization of analyses, and drafting of the original manuscript. S.T.M.: Investigation, experimental work, validation. S.O.O.: Supervision, resources, review, and editing of the final draft, corresponding author. All authors have read and agreed to the published version of the manuscript.

Data Availability Statement: Data available as Supplementary Materials.

Conflicts of Interest: The authors declare no conflict of interest.

References

1. Cornils, B.; Herrmann, W.A. Concepts in homogeneous catalysis: The industrial view. *J. Catal.* **2003**, *216*, 23–31. [CrossRef]
2. Wang, L.; Yang, Q.; Chen, H.; Li, R.-X. A novel cationic dinuclear ruthenium complex: Synthesis, characterization and catalytic activity in the transfer hydrogenation of ketones. *Inorg. Chem. Commun.* **2011**, *14*, 1884–1888. [CrossRef]
3. Noyori, R.; Hashiguchi, S. Asymmetric Transfer Hydrogenation Catalyzed by Chiral Ruthenium Complexes. *Acc. Chem. Res.* **1997**, *30*, 97–102. [CrossRef]
4. Foubelo, F.; Najera, C.; Yus, M. Catalytic asymmetric transfer hydrogenation of ketones: Recent advances. *Tetrahedron Asymmetry* **2015**, *26*, 769–790. [CrossRef]
5. Aydemir, M.; Durap, F.; Baysal, A.; Meric, N.; Buldağ, A.; gümgüm, B.; Özkar, S.; Yıldırım, L.T. Novel neutral phosphinite bridged dinuclear ruthenium (II) arene complexes and their catalytic use in transfer hydrogenation of aromatic ketones: X-ray structure of a new Schiff base, N3, N3′-di-2-hydroxybenzylidene-[2, 2′] bipyridinyl-3, 3′-diamine. *J. Mol. Catal. A Chem.* **2010**, *326*, 75–81. [CrossRef]
6. Pye, D.R.; Mankad, N.P. Bimetallic catalysis for C–C and C–X coupling reactions. *Chem. Sci.* **2017**, *8*, 1705–1718. [CrossRef]
7. Liu, T.; Chai, H.; Wang, L.; Yu, Z. Exceptionally Active Assembled Dinuclear Ruthenium (II)-NNN Complex Catalysts for Transfer Hydrogenation of Ketones. *Organometallics* **2017**, *36*, 2914–2921. [CrossRef]
8. Wang, D.; Astruc, D. The golden age of transfer hydrogenation. *Chem. Rev.* **2015**, *115*, 6621–6686. [CrossRef]
9. Chai, H.; Wang, Q.; Liu, T.; Yu, Z. Diruthenium (II)–NNN pincer complex catalysts for transfer hydrogenation of ketones. *Dalton Trans.* **2016**, *45*, 17843–17849. [CrossRef]
10. Yoshida, K.; Kamimura, T.; Kuwabara, H.; Yanagisawa, A. Chiral bicyclic NHC/Ir complexes for catalytic asymmetric transfer hydrogenation of ketones. *Chem. Commun.* **2015**, *51*, 15442–15445. [CrossRef]
11. Volpe, A.; Baldino, S.; Tubaro, C.; Baratta, W.; Basato, M.; graiff, C. Dinuclear Di (N-heterocyclic carbene) Iridium (III) Complexes as Catalysts in Transfer Hydrogenation. *Eur. J. Inorg. Chem.* **2016**, *2016*, 247–251. [CrossRef]
12. Ashley, J.M.; Farnaby, J.H.; Hazari, N.; Kim, K.E.; Luzik, E.D., Jr.; Meehan, R.E.; Meyer, E.B.; Schley, N.D.; Schmeier, T.J.; Tailor, A.N. Axially chiral dimeric Ir and Rh complexes bridged by flexible NHC ligands. *Inorg. Chim. Acta* **2012**, *380*, 399–410. [CrossRef]
13. Madern, N.; Talbi, B.; Salmain, M. Aqueous phase transfer hydrogenation of aryl ketones catalysed by achiral ruthenium (II) and rhodium (III) complexes and their papain conjugates. *Appl. Organomet. Chem.* **2013**, *27*, 6–12. [CrossRef]
14. Dayan, O.; Çetinkaya, B. Mono-and binuclear ruthenium (II) complexes containing pyridine-2, 6-diimine (Pydim) ligands: Synthesis, characterization and catalytic activity in the transfer hydrogenation of acetophenone. *J. Mol. Catal. A: Chem.* **2007**, *271*, 134–141. [CrossRef]
15. Nath, B.D.; Takaishi, K.; Ema, T. Macrocyclic multinuclear metal complexes acting as catalysts for organic synthesis. *Catal. Sci. Technol.* **2020**, *10*, 12–34. [CrossRef]
16. Maity, A.; Sil, A.; Patra, S.K. Ruthenium (II) Complexes of 4′-(Aryl)-2, 2′: 6′, 2″-terpyridyl Ligands as Simple Catalysts for the Transfer Hydrogenation of Ketones. *Eur. J. Inorg. Chem.* **2018**, *2018*, 4063–4073. [CrossRef]
17. Bratko, I.; gomez, M. Polymetallic complexes linked to a single-frame ligand: Cooperative effects in catalysis. *Dalton Trans.* **2013**, *42*, 10664–10681. [CrossRef] [PubMed]
18. Liu, T.; Wu, K.; Wang, L.; Fan, H.; Zhou, Y.-G.; Yu, Z. Assembled multinuclear ruthenium (II)–NNNN complexes: Synthesis, catalytic properties, and DFT calculations. *Organometallics* **2019**, *39*, 93–104. [CrossRef]
19. Kumah, R.T.; Vijayan, P.; Ojwach, S.O. Carboxamide carbonyl-ruthenium (ii) complexes: Detailed structural and mechanistic studies in the transfer hydrogenation of ketones. *New J. Chem.* **2022**. [CrossRef]
20. Yadav, S.; Vijayan, P.; Yadav, S.; gupta, R. Ruthenium complexes of phosphine–amide based ligands as efficient catalysts for transfer hydrogenation reactions. *Dalton Trans.* **2021**, *50*, 3269–3279. [CrossRef]

21. Arafa, W.A. Sonochemical Preparation of Dipicolinamide Mn-complexes and Their Application as Catalysts Towards Sono-synthesis of Ketones. *J. Heterocycl. Chem.* **2019**, *56*, 1403–1412. [CrossRef]

22. Meghdadi, S.; Mereiter, K.; Amirnasr, M.; Karimi, F.; Amiri, A. Synthesis, crystal structure and electrochemistry of cobalt (III) carboxamide complexes with amine and azide ancillary ligands. *Polyhedron* **2014**, *68*, 60–69. [CrossRef]

23. Meghdadi, S.; Mereiter, K.; Shams Mohammadi, N.; Amiri, A. Synthesis, characterization and X-ray crystal structure of a cobalt (III) complex with 2-bis (pyridine-2-carboxamido)-4, 5-dimethylbenzene ligand. *Inorg. Chem. Res.* **2017**, *1*, 69–78.

24. Aradhyula, B.P.R.; Kaminsky, W.; Kollipara, M.R. Half-sandwich d^6 metal complexes with bis (pyridine carboxamide) benzene ligand: Synthesis and spectral analysis. *J. Mol. Struct.* **2017**, *1149*, 162–170. [CrossRef]

25. Almodares, Z.; Lucas, S.J.; Crossley, B.D.; Basri, A.M.; Pask, C.M.; Hebden, A.J.; Phillips, R.M.; McGowan, P.C. Rhodium, iridium, and ruthenium half-sandwich picolinamide complexes as anticancer agents. *Inorg. Chem.* **2014**, *53*, 727–736. [CrossRef] [PubMed]

26. Meghdadi, S.; Amirnasr, M.; Kiani, M.; Fadaei Tirani, F.; Bagheri, M.; Schenk, K.J. Benign synthesis of quinolinecarboxamide ligands, H2bqbenzo and H2bqb and their Pd (II) complexes: X-ray crystal structure, electrochemical and antibacterial studies. *J. Coord. Chem.* **2017**, *70*, 2409–2424. [CrossRef]

27. Allen, F.H. The Cambridge Structural Database: A quarter of a million crystal structures and rising. *Acta Crystallogr. Sect. B Struct. Sci.* **2002**, *58*, 380–388. [CrossRef]

28. Botubol-Ares, J.M.; Cordón-Ouahhabi, S.; Moutaoukil, Z.; Collado, I.G.; Jiménez-Tenorio, M.; Puerta, M.C.; Valerga, P. Methylene-Linked Bis-NHC Half-Sandwich Ruthenium Complexes: Binding of Small Molecules and Catalysis toward Ketone Transfer Hydrogenation. *Organometallics* **2021**, *40*, 792–803. [CrossRef]

29. Wasylenko, D.J.; ganesamoorthy, C.; Henderson, M.A.; Koivisto, B.D.; Osthoff, H.D.; Berlinguette, C.P. Electronic modification of the [RuII (tpy)(bpy)(OH2)] 2+ scaffold: Effects on catalytic water oxidation. *J. Am. Chem. Soc.* **2010**, *132*, 16094–16106. [CrossRef]

30. Pospech, J.; Fleischer, I.; Franke, R.; Buchholz, S.; Beller, M. Alternative metals for homogeneous catalyzed hydroformylation reactions. *Angew. Chem. Int. Ed.* **2013**, *52*, 2852–2872. [CrossRef]

31. Pachisia, S.; Kishan, R.; Yadav, S.; gupta, R. Half-Sandwich Ruthenium Complexes of Amide-Phosphine Based Ligands: H-Bonding Cavity Assisted Binding and Reduction of Nitro-substrates. *Inorg. Chem.* **2021**, *60*, 2009–2022. [CrossRef] [PubMed]

32. Yadav, S.; Vijayan, P.; gupta, R. Ruthenium complexes of N/O/S based multidentate ligands: Structural diversities and catalysis perspectives. *J. Organomet. Chem.* **2021**, *954*, 122081. [CrossRef]

33. Govindaswamy, P.; Canivet, J.m.; Therrien, B.; Süss-Fink, g.; Štěpnička, P.; Ludvík, J. Mono and dinuclear rhodium, iridium and ruthenium complexes containing chelating 2, 2′-bipyrimidine ligands: Synthesis, molecular structure, electrochemistry and catalytic properties. *J. Organomet. Chem.* **2007**, *692*, 3664–3675. [CrossRef]

34. Viji, M.; Tyagi, N.; Naithani, N.; Ramaiah, D. Aryl appended neutral and cationic half-sandwich ruthenium (ii)–NHC complexes: Synthesis, characterisation and catalytic applications. *New J. Chem.* **2017**, *41*, 12736–12745. [CrossRef]

35. Meriç, N.; Durap, F.; Aydemir, M.; Baysal, A. The application of tunable tridentate P-based ligands for the Ru (II)-catalysed transfer hydrogenation of various ketones. *Appl. Organomet. Chem.* **2014**, *28*, 803–808. [CrossRef]

36. Raja, N.; Ramesh, R. Binuclear ruthenium (II) pyridazine complex catalyzed transfer hydrogenation of ketones. *Tetrahedron Lett.* **2012**, *53*, 4770–4774. [CrossRef]

37. Martins, J.E.; Clarkson, g.J.; Wills, M. Ru (II) complexes of N-alkylated TsDPEN ligands in asymmetric transfer hydrogenation of ketones and imines. *Org. Lett.* **2009**, *11*, 847–850. [CrossRef]

38. Wang, Q.; Chai, H.; Yu, Z. Dimeric ruthenium (II)-NNN complex catalysts bearing a pyrazolyl-pyridylamino-pyridine ligand for transfer hydrogenation of ketones and acceptorless dehydrogenation of alcohols. *Organometallics* **2017**, *36*, 3638–3644. [CrossRef]

39. Armarego, W.L. Purification of Laboratory Chemicals. Butterworth-Heinemann: Oxford, UK, 2017.

40. Fulmer, g.R.; Miller, A.J.; Sherden, N.H.; gottlieb, H.E.; Nudelman, A.; Stoltz, B.M.; Bercaw, J.E.; goldberg, K.I. NMR chemical shifts of trace impurities: Common laboratory solvents, organics, and gases in deuterated solvents relevant to the organometallic chemist. *Organometallics* **2010**, *29*, 2176–2179. [CrossRef]

41. Sheldrick, g.M. Crystal structure refinement with SHELXL. *Acta Crystallogr. Sect. Cs Struct. Chem.* **2015**, *71*, 3–8. [CrossRef]

42. Karaca, E.Ö. The catalytic activity of new iridium(I) N-heterocyclic carbene complexes for hydrogen transfer reaction of ketones. *Mon. Für Chem. Chem. Mon.* **2021**, *152*, 287–293. [CrossRef]

43. Bernier, C.M.; Merola, J.S. Design of Iridium N-Heterocyclic Carbene Amino Acid Catalysts for Asymmetric Transfer Hydrogenation of Aryl Ketones. *Catalysts* **2021**, *11*, 671. [CrossRef]

44. Yoshida, M.; Hirahata, R.; Inoue, T.; Shimbayashi, T.; Fujita, K.-i. Iridium-catalyzed transfer hydrogenation of ketones and aldehydes using glucose as a sustainable hydrogen donor. *Catalysts* **2019**, *9*, 503. [CrossRef]

45. Wang, R.; Han, X.; Xu, J.; Liu, P.; Li, F. Transfer Hydrogenation of Ketones and Imines with Methanol under Base-Free Conditions Catalyzed by an Anionic Metal–Ligand Bifunctional Iridium Catalyst. *J. Org. Chem.* **2020**, *85*, 2242–2249. [CrossRef] [PubMed]